*Journal of Geography and Cartography* 2025, 8(4), 11738.
https://doi.org/10.24294/jgc11738

Article

# Assessments on biomass production by remote sensing

**Ana Azevedo[1], Antônio Teixeira[1,*], Inajá Sousa[1], Janice Leivas[2], Celina Takemura[2]**

[1] Federal University of Sergipe Water Resources Post-Graduation Program, São Cistóvão 49100, SE, Brazil
[2] Embrapa Territory, Research Department, Campinas 13015, SP, Brazil
*** Corresponding author:** Antônio Teixeira, heribertoteixeira11@gmail.com

**CITATION**

Azevedo A, Teixeira A, Sousa I, et al. (2025). Assessments on biomass production by remote sensing. Journal of Geography and Cartography. 8(4): 11738. https://doi.org/10.24294/jgc11738

**ARTICLE INFO**

Received: 6 May 2025
Accepted: 16 June 2025
Available online: 26 December 2025



**Abstract:** Biomass production (BIO) and its anomalies were modeled using MODIS satellite images and gridded weather data to test an environmental monitoring system in the biomes Atlantic Forest (AF) and Caatinga (CT) within SEALBA, an agricultural growing region bordered by the states of Sergipe (SE), Alagoas (AL), and Bahia (BA), Northeast Brazil. Spatial and temporal variations on BIO between these biomes were strongly identified, with the annual long-term averages (2007–2023) for AF and CT of 78 ± 22 and 58 ± 17 kg ha$^{-1}$ d$^{-1}$, respectively. BIO anomalies were detected through its standardized indexes—STD ($BIO_{STD}$), comparing the results for the years from 2020 to 2023 with the long-term rates from 2007 to each of these years. The highest negative $BIO_{STD}$ values were in 2023, but concentrated in CT, indicating periods with the lowest vegetation growth, regarding the long-term conditions from 2007 to 2023. The largest positive $BIO_{STD}$ values were for the AF biome in 2022, evidencing the highest vegetative vigor in comparison with the long-term period 2007–2022. The proposed BIO monitoring system is important for environmental policies as they picture suitable periods and places for agricultural and forestry explorations, allowing sustainable managements under climate and land-use changes conditions, with possibilities for replication of the methods in other environmental conditions.

**Keywords:** geotechnologies; environmental management; land-use changes; Atlantic Forest; Caatinga

## 1. Introduction

Biomass production (BIO) is a robust environmental indicator for agroecosystems of any biome [1] (Wu et al., 2010), being its values highly variable in both space and time [2–5] (Adak et al., 2013; Teixeira et al., 2023; Yan et al., 2009, Bayma et al., 2025). Under water scarcity conditions, particularly in semiarid and arid regions, the challenge is BIO improvements through optimized management practices [2] (Adak et al., 2013). Monitoring the vegetation growth is critical for ecological equilibrium [6–9] (Yang et al., 2016; Zhang & Zhang, 2019; Zang et al., 2019, 2021) and this task requires large-scale studies to guide sustainable exploration of land and water resources [10–12] (Almeida et al., 2023; Santos et al., 2020; Zhang et al., 2022). Quantifying BIO can be also useful to analyze the feasibility of setting up new biomass power plants and to optimize the best locations for agriculture expansion [13] (Shi et al., 2008). Many promised pathways for raising BIO in distinct agroecosystems are available over the continuum from forests and fully rainfed to fully irrigated farming systems [14] (Molden et al., 2007). BIO is associated with photosynthetically active radiation (PAR) that is part of the short-wave solar radiation which is absorbed by chlorophyll for photosynthesis in vegetation, regulating primary productivity, or the rate of carbon fixed by the plants. Under climate and land use changes, the joint use

of remote sensing and weather data are suitable tools for monitoring BIO, supporting public policies for the rational environmental managements [3,15–17] (Clementini et al., 2020, Chen et al., 2021; Rampazo et al., 2020; Teixeira et al., 2023). Applications of remote sensing with satellite images, at different temporal and spatial scales, also allow the detection of BIO anomalies for specific periods along the year [8,9,18–22] (Beguería et al., 2014; Bento et al., 2018; Gouveia et al., 2017; Teixeira et al., 2021; Vicente-Serrano et al., 2018; Zhang et al., 2019; Zhang et al., 2021).

Standardized indices for detecting large-scale anomalies have been generally based on evapotranspiration studies [22,23] (Kim and Rhee 2016; Vicente-Serrano et al. 2018). Considering vegetation, the Normalized Difference Vegetation Index (NDVI) has been widely used to indicate variations in soil cover by plants [19,24] (Bento et al. 2018; Brouwers et al. 2015). This index was developed to describe the probability of variation in NDVI from its normal value over a long period of data [25]. However, to reflect environmental stress on vegetation, NDVI values have delayed responses, regarding the root-zone moisture responses [8] (Zhang et al., 2019). Standardized indices have been also based on precipitation (P), evapotranspiration (ET), and soil moisture [9,22,26] (Hao & AghaKouchak, 2013; Vicente-Serrano et al., 2018; Zhang et al., 2021). However, besides NDVI, P and ET, other parameters derived from remote sensing measurements are important, such as BIO, which is a robust indicator of water and vegetation conditions, important for environmental monitoring [3,21] (Teixeira et al., 2021, 2023). ET anomaly quantifications in semi-arid regions are considered appropriate [23] (Vicente-Serrano et al., 2018), as water stress affects BIO [27] (Zhang et al., 2016). Thus, an accurate assessment of environmental impacts on vegetation activity is crucial for understanding the response of the agroecosystems to anomalies [8,9] (Zhang et al., 2019, 2021), especially under environmental constraints impacting BIO, as in case of some Brazilian Northeast areas.

The replacement of natural species by agricultural crops promotes carbon sinks, affecting BIO [28] (Ceschia et al., 2010), while water stress increases can drop vegetation vigor [29] (Zhao & Running, 2010). Monitoring the dynamics of these effects along the years is essential for agricultural and forestry explorations to assess the dimension of environmental impacts [3,6,7,21] (Teixeira et al., 2021, 2023; Yang et al., 2016; Zhang & Zhang, 2019). In some biomes of Northeast Brazil, there are several plant species suffering environmental impacts that affect BIO, including land use changes [30,31] (Lewinsohn & Prado, 2005 Mariano et al., 2018), as in case of SEALBA, an agricultural growing region involving the states of Sergipe (SE), Alagoas (AL) and Bahia (BA). This region has different types of species from the Caatinga (CT) and Atlantic Forest (FA) biomes being replaced by agricultural crops, demanding large-scale studies to support these land-use changes [32–34] (Ribeiro et al., 2009; Santos et al., 2014; Silva et al., 2017). The use of long-term remote sensing and weather data throughout standardized indices based on BIO is suitable for policy decision making under these unstable conditions. Some field studies about water availability and vegetation growth were carried out in the Brazilian AF and CT biomes [34–37] (Marques et al., 2020; Pereira et al., 2010; Silva et al., 2017; Teixeira et al. 2008). However, few efforts have been made to monitor BIO over the years within these biomes considering a large data series for average conditions, allowing to monitor anomalies for specific periods. These assessments can help to understand the

responses of natural vegetation and agricultural crops to environmental impacts under climate and land use changes scenarios [38] (Reinermann et al., 2020).

For BIO assessments in the current research, the radiation efficiency concept (RUE) devised, based on radiation interception, was applied [3,39] (Claverie et al., 2012; Teixeira et al., 2023). This interception is variable throughout the year and during the crop growing periods [40] (Tesfaye et al., 2006). The RUE Monteith's model proposes a direct proportional relation between BIO and the amount of photosynthetically active radiation absorbed by the vegetation canopies [41] (Monteith, 1977). Although uncertainties in the radiation efficiency values, due to their spatiotemporal variations [42] (Zhao et al., 2010), the RUE model accuracy has been considered acceptable for remote sensing applications with satellite data [43–45] (Bastiaanssen & Ali, 2003; Nyoley et al., 2019; Zwart et al., 2010). To include the effect of root-zone moisture on BIO rates, through the evaporative fraction - $ET_f$, i.e. the ratio of actual ($ET_a$) to reference ($ET_0$) evapotranspiration, we used the SAFER (Simple Algorithm for Evapotranspiration Retrieving) algorithm which was developed in Northeast Brazil by using simultaneous field and remote sensing measurements to estimate the water and vegetation parameters in agricultural crops and natural vegetation. Bands 1 to 7 from Landsat 5 satellite; and bands 1, 2, 31 and 32 from MODIS sensor were used together with micrometeorological data, to derive and validate all the SAFER's equations [46,47] (Teixeira, 2010; 2013). The algorithm can be applied together with the RUE model to satellite images. An important advantage of SAFER, regarding other algorithms, is that it can be used without thermal bands, being possible to use only the visible and near infrared spectrum, more easily available [48] (Consoli & Vanella, 2014). In addition, the thermal bands of the MODIS, sensor, with a spatial resolution of 1 km, means that the images should cover more mixed agroecosystem types, when comparing with the 250-m spatial resolution of its red and near infrared bands used in current research [3,47] (Teixeira et al., 2013, 2023).

The remote sensing derived parameters crossed with weather data involved in the modelling steps were the Normalized Different Vegetation Index (NDVI), surface albedo ($\alpha_0$) and surface temperature ($T_0$), considered BIO driven physical parameters. Pixel values of NDVI, $\alpha_0$ and $T_0$ were used to model $ET_f$. In the current research, without thermal satellite bands, $T_0$ was retrieved from the radiation balance applying the Stefan Boltzmann low assuming the low atmosphere and the Earth surface emitting longwave radiation as back bodies [3] (Teixeira et al., 2023). To implement a BIO monitoring system taking the SEALBA agricultural growing region as a reference, we tested the joint use of the RUE model with the SAFER algorithm, with MODIS MOD13Q1 reflectance products and long-term weather data from 2007 to 2023 at the same satellite 16-day timescales, to retrieve BIO dynamics throughout the years. Besides characterizing long-term conditions, we used a standardized index based on BIO ($BIO_{STD}$) for further anomaly assessments on vegetation vigor for specific periods of the last four years of this long-term data set. The authors believe that the success of applications for this specific Brazilian region may stimulate replications of the methodology in other environmental conditions, even in other countries, only calibrating the BIO modelling equations.

## 2. Material and methods

### 2.1. Study area and data set

**Figure 1** shows the location of SEALBA in Northeast of Brazil with its limits in the states of Sergipe—SE, Alagoas—AL and Bahia—BA (**Figure 1a**); the weather stations, highlighting the altitudes (**Figure 1b**); and the Atlantic Forest—AF and Caatinga—CT biomes (**Figure 1c**).

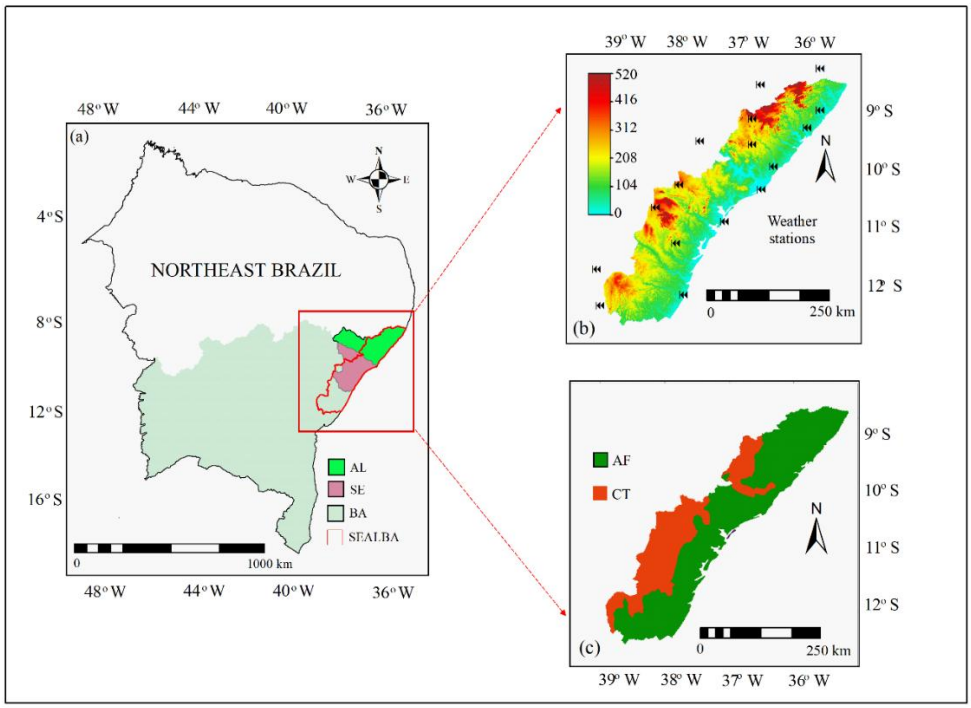


**Figure 1.** Location of the SEALBA agricultural growing region in Northeast Brazil involving the states of Sergipe—SE, Alagoas—AL and Bahia—BA (**a**); weather stations, highlighting altitudes (**b**); and the Atlantic Forest—AF and Caatinga—CT biomes (**c**).

The 16 weather stations used were from the National Meteorological Institute (INMET—https://www.gov.br/agricultura/pt-br/assuntos/inmet), while classification into AF and CT biomes was according to the Geographic and Statistical Brazilian Institute (IBGE—www.ibge.gov.br). Being the MODIS pixel size of 250 m, the SEALBA region with 6.2 Mha (**Figure 1a**), involves the AF and CT biomes. The AF areas, mostly below 275 m of altitude, are in a portion closer to the coastline, while CT areas are located more to the west side, being the majority above 275 m of altitude (**Figure 1b,c**).

The AF biome, with a humid tropical climate, characterized by forest vegetation, comprises dense and open rain forests, semi-decidual season forests and ecosystems associate to coastal lowlands [49] (Procopio et al., 2019). The climate is tropical humid but with mixed microclimates involving natural and anthropized areas [32] (Ribeiro et al., 200). Its environmental conditions are influenced by air masses coming from the Atlantic Ocean, which increase air temperature and air humidity, with rainfall well distributed throughout the year. Average annual temperatures range from 13 to 27 °C; annual rainfall from 1000 to 2500 mm with the rainy season concentrated from

December to March [49,50] (Francisquini et al., 2020; Procopio, 2019). The CT biome is composed of trees and shrubs with structures to overcome environmental stress conditions, with plants presenting resilience under increasing dryness. Its climate is characterized by distinct wet and dry seasons, with a short rainy period (3–5 months, typically January–May) and a prolonged dry season (7–9 months, June–December). Average annual rainfall varies from 300 to 1000 mm and average temperatures range from 25 °C to 30 °C promoting aridity conditions, however, plant species have been adapted to these dry conditions with leaves modified into thorns, thick bark, and leaf losses [49,33,51] (Almagro et al., 2017; Procopio, 2019; Santos et al., 2014). The adopted criteria for the agricultural aptitude in SEALBA was rainfall above 450 mm from April to September in at least 50% of each county inside the region, and under this condition, natural vegetation of both biomes has been replaced by agricultural crops, such as grains, fruit trees, sugar cane, forestry and pasture, where the relief is predominantly soft wave, with slope between 3% and 8% [49].

The input weather data for BIO modeling came from 16 stations (**Figure 1b**), being global incident solar radiation ($R_G$) and air temperature ($T_a$), covering the entire SEALBA region, enabling interpolation through a geographic information system (GIS), using the geostatistical "average movement" method, which resulted in pixels with the same spatial resolution of that for the MODIS images. Additional data on relative humidity (RH) and wind speed (u) were used with $R_G$ and $T_a$ to calculate reference evapotranspiration ($ET_0$) according to [52] Allen et al. (1998), which together with precipitation (P) were used for climate characterization of the study region regarding the long-term conditions from 2007 to 2023.

The bands 1 (red) and 2 (infrared) from the MODIS sensor (MOD13Q1 reflectance product) were downloaded from the site of EARTHDATA Aρρ EEARS (https://lpdaacsvc.cr.usgs.gov/appeears/) and used together with the gridded weather data. The images have spatial and temporal resolutions of 250 m and 16 days, respectively, giving 23 free-cloud images in a year [3] (Teixeira et al., 2023). The MOD13Q1 product provides the NDVI and the Enhanced Vegetation Index (EVI). The algorithm chooses the best available pixel value from all the acquisitions from the 16-day periods. The criteria used are low clouds, low view angle, and the highest NDVI/EVI value. Along with these vegetation layers, the HDF file has reflectance bands 1 and 2, used in the current research.

Considering the long-term period from 2007 to 2023, it was possible to quantify anomalies for specific years from 2020 to 2023, in the AF and CT biomes within the SEALBA agricultural growing region. To retrieve BIO from all MODIS images and gridded $R_G$ and $T_a$ data, the SAFER's equations were applied by using a script built in a geographic information system (GIS).

## 2.2. Modeling biomass production and its anomalies

**Figure 2** presents the flowchart for modeling BIO and its anomalies coupling the RUE model and the SAFER algorithm.

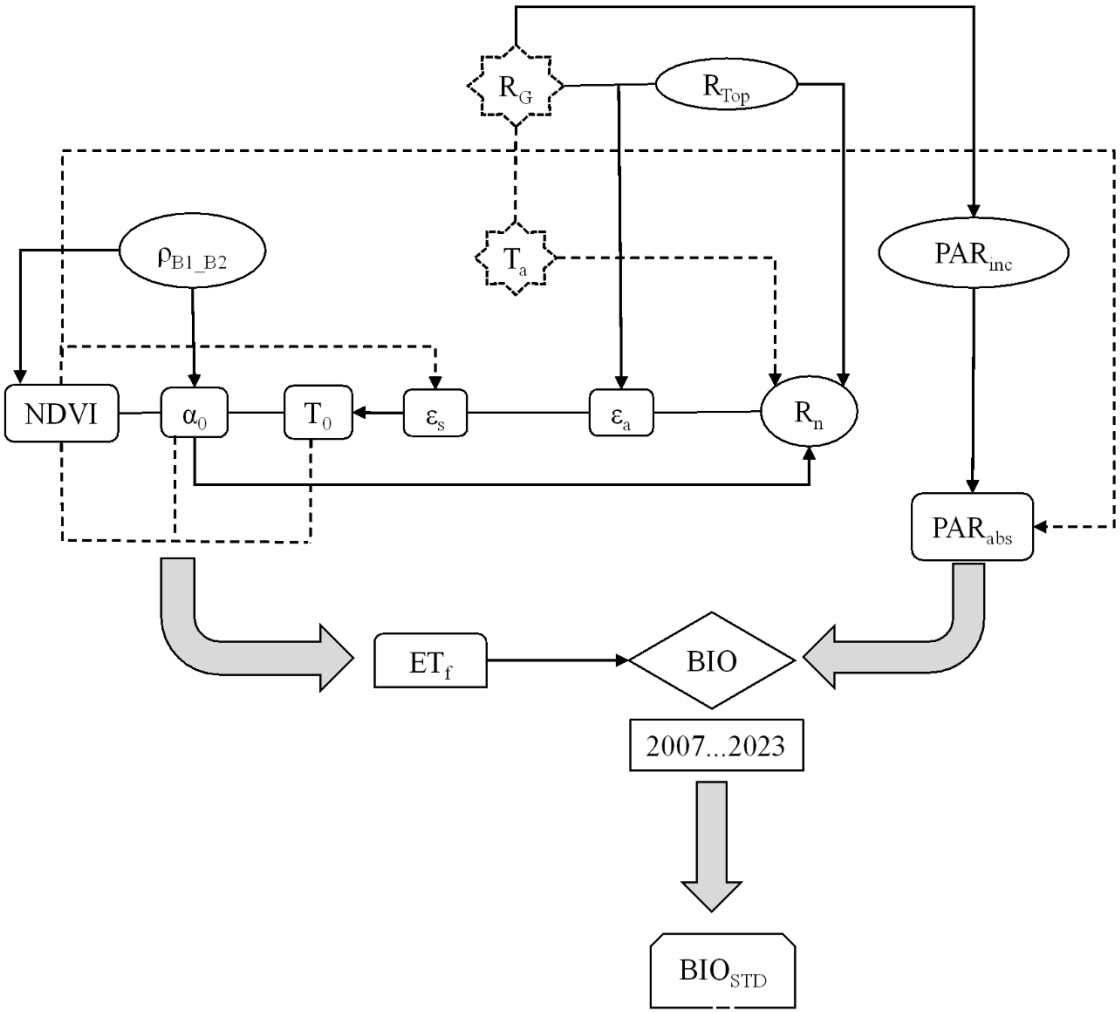


**Figure 2.** Flowchart for modelling biomass production (BIO) and its anomalies through the standardized index—STD ($BIO_{SPD}$) by applying the RUE model and the SAFER algorithm with gridded data on global solar radiation ($R_G$) and mean air temperature ($T_a$).

The regression coefficients of the equations involved in the modelling steps (**Figure 2**) were previously obtained in the Northeast region of Brazil with simultaneous field and satellite measurements of the energy and carbon components, detailed in [37,46,47]Teixeira (2010) and Teixeira et al. (2008, 2013), and they can be calibrated for distinct environmental conditions following the procedures described in these previous papers. In addition, acquiring $T_0$ as residue in the radiation balance gives mutual compensation, reducing possible errors in this model input parameter, as in the upward and downward long-wave fluxes, they are self-canceling. The SAFER algorithm was elaborated and validated with Landsat images when it was first called PM2 [46] (Teixeira, 2010). Later, it was also calibrated and validated in several agroecosystems under different environmental environments [10,11,21] (Almeida et al., 2023; Teixeira et al., 2021; Santos et al. 2020). On the other hand, the regression coefficients for the BIO model were previously calibrated involving distinct vegetated surfaces by [43] Bastiaanssen and Ali (2003) and applied in the Brazilian biomes for

actual and long-term conditions [3,5,17,21] (Bayma et al., 2025; Rampazo et al., 2023; Teixeira et al., 2021, 2023).

Thus, with previous calibrations and validations of the models, together with assumptions based on physical processes in the current paper, one can expect sufficient accuracy for BIO evaluations and comparisons among the biomes in the SEALBA conditions, being not strictly necessary new expensive validations with field data.

**2.2.1. Normalized difference vegetation index (NDVI) and surface albedo ($\alpha_0$)**

After clipping the MODIS reflectance images for the SEALBA region, the Normalized Difference Vegetation Index (NDVI) was calculated and incorporated in the BIO modelling steps as a surface cover and root-zone moisture remote-sensing indicator [25] (Peters et al., 2002):

$$\mathrm{NDVI} = \frac{\rho_2 - \rho_1}{\rho_2 + \rho_1} \tag{1}$$

where $\rho_1$ and $\rho_2$ are the reflectances in bands 1 (red) and 2 (near infrared) coming from the MODIS sensor.

The surface albedo ($\alpha_0$) values were calculated as:

$$\alpha_0 = a + b\rho_1 + c\rho_2 \tag{2}$$

where a, b and c are regression coefficients of 0.08, 0.41, and 0.14 for Northeast Brazil [47] (Teixeira et al., 2013).

**2.2.2. Surface temperature ($T_0$)**

The net radiation ($R_n$) was estimated by using the Slob equation [53] (de Bruin et al., 1987):

$$R_n = (1 - \alpha_0) R_G - a_L \tau_{sw} \tag{3}$$

where $\tau_{sw}$ is the atmospheric transmissivity for short wavelengths considered as the ratio between $R_G$ and the radiation incident at the top of the atmosphere ($R_{TOP}$) being L a regression coefficient as a function of $T_a$ [37] (Teixeira et al., 2008).

The atmospheric emissivity ($\varepsilon_a$) was calculated by:

$$\varepsilon_a = a_A \left(\ln \tau_{sw}\right)^{b_A} \tag{4}$$

where $a_A$ and $b_A$ are the regression coefficients 0.94 and 0.11, respectively for Northeast Brazil [46] (Teixeira, 2010).

The surface emissivity ($\varepsilon_s$) was estimated according to [10] Almeida et al. (2023):

$$\varepsilon_s = a_0 \ln \mathrm{NDVI} + b_0 \tag{5}$$

where $a_0$ and $b_0$ are the regression coefficients 0.06 and 1.00, respectively, for Northeast Brazil.

Using the residual method, surface temperature ($T_0$) was estimated using the Stefan-Boltzmann law:

$$T_0 = \frac{\sqrt[4]{R_G\left(1-\alpha_0\right)+\sigma\varepsilon_a T_a^{\,4}-R_n}}{\sigma\varepsilon_s} \tag{6}$$

where is $\sigma = 5.67\ 10^{-8}\ W\ m^{-2}\ K^{-4}$ is the Stefan-Boltzmann constant [17] (Rampazo et al., 2020).

### 2.2.3. Biomass production (BIO)

To include root-zone moisture conditions in BIO calculations, the evapotranspiration fraction ($ET_f$), i.e., the ratio of actual (ET) to reference evapotranspiration ($ET_0$), was modeled by the SAFER equation [54] (Venancio et al., 2021):

$$ET_f = \exp\left[a_{sf} + b_{sf}\left(\frac{T_0}{\alpha_0 NDVI}\right)\right] \tag{7}$$

where $a_{sf}$ and $b_{sf}$ are the regression coefficients 1.80 and −0.008, respectively, for Northeast Brazil.

To estimate the incident photosynthetically active radiation ($PAR_{inc}$), it was considered as a fraction of $R_G$ [21] (Teixeira et al., 2023):

$$PAR_{inc} = a_R R_G \tag{8}$$

where the regression coefficient $a_R$ used was 0.44 in Northeast Brazil.

The values of the absorbed photosynthetically active radiation ($PAR_{abs}$) were calculated according to [43] Bastiaanssen & Ali (2003):

$$PAR_{abs} = f_{PAR} PAR_{inc} \tag{9}$$

where the factor $f_{PAR}$ was estimated from NDVI (Bayma et al., 2025):

$$f_{PAR} = a_P NDVI + b_P \tag{10}$$

where $a_P$ and $b_P$ are regression coefficients considered as 1.257 and −0.161, respectively.

BIO was then quantified using the RUE model [41] (Monteith, 1977) as:

$$BIO = \varepsilon_{max} ET_f PAR_{abs} 0,864 \tag{11}$$

where $\varepsilon_{max}$ is the maximum light use efficiency, which for the majority of C3 plants in SEALBA was assumed to be 2.45 g $MJ^{-1}$, and 0.864 is a conversion factor.

### 2.2.4. Standardized index for the biomass production ($BIO_{STD}$)

To determine BIO anomalies, considering the annual and 16-day periods of the MODIS MOD13Q1 product, the standardized index equation below was used [9,21,55] (Leivas et al., 2014; Teixeira et al., 2021, Zhang et al., 2021):

$$BIO_{STD} = \frac{BIO - BIO_{mean}}{SD} \tag{12}$$

where $BIO_{STD}$ is the standardized index for biomass production (16-day or year timescales, from 2020 to 2023), BIO is the long-term averages for the specific periods (2007–2020, 2007–2021, 2007–2022, and 2007–2023), $BIO_{mean}$ is the long-term average and SD is the pixel-by-pixel standard deviation for these periods.

## 3. Results

### 3.1. Long-term weather drivers

The most important weather drivers' parameters for BIO are precipitation (P), reference evapotranspiration ($ET_0$), incident global solar radiation ($R_G$) and air temperature ($T_a$). **Figure 3** shows their long-term average pixel values for the period from 2007 to 2023, together with the standard deviations (SD), at the 16-day timescales of the MOD13Q1 reflectance product, in terms of Day of the Year (DOY), classifying the Atlantic Forest (AF) and Caatinga (CT) biomes within SEALBA.

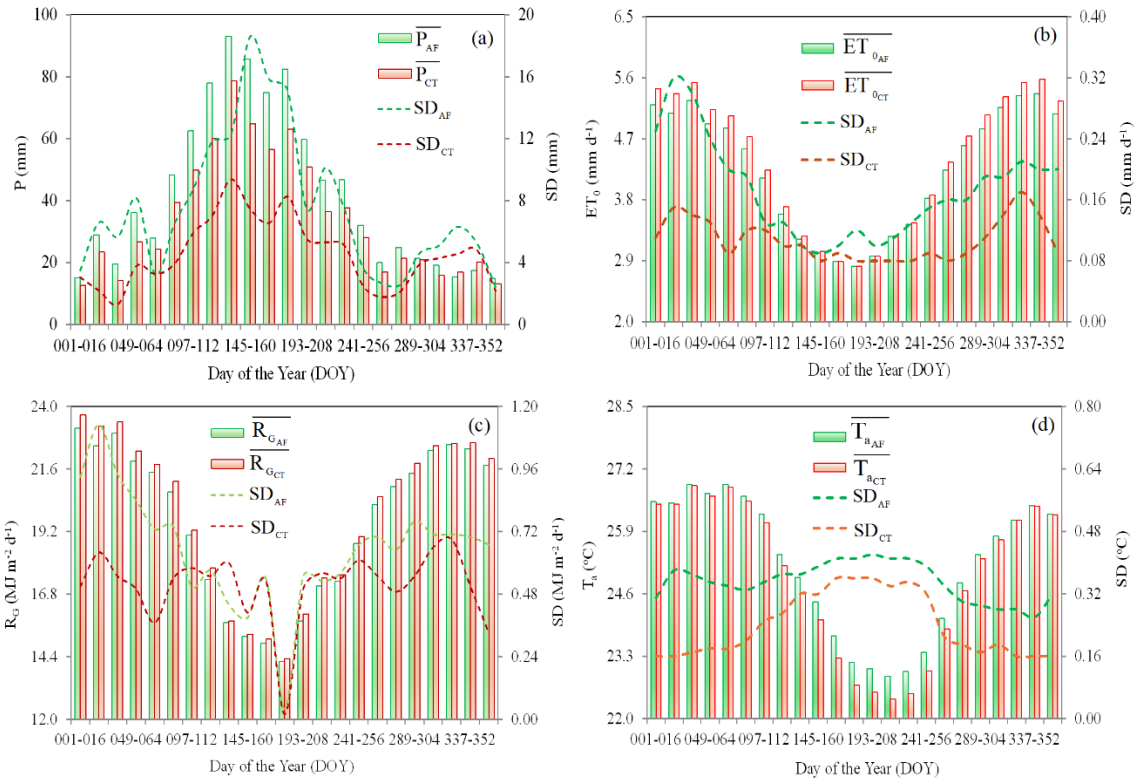


**Figure 3.** Long-term average pixel values and standard deviations (SD) of weather BIO drivers: (**a**) precipitation (P), (**b**) reference evapotranspiration ($ET_0$), (**c**) incident global solar radiation ($R_G$) and (**d**) average air temperature ($T_a$), at the 16-day MOD13Q1 product, for the biomes Atlantic Forest (AF) and Caatinga (CT) within SEALBA, in terms of Day of the Year (DOY), regarding the period from 2007 to 2023. Overbars means average pixel values.

From **Figure 3a**, it is noticed that rainfalls are concentrated in the middle of the year for both biomes, AF and CT, with higher amounts in AF. The highest P values are between April and July (DOY 097–208), when the mean 16-day total is above 60 mm for AF and larger than 50 mm for CT. The lowest ones, with mean 16-day totals below 20 mm in both biomes, are from November to January (DOY 305–016), limiting somewhat BIO rates. At the annual scale, P accounting 781 mm $yr^{-1}$ in CT, is 82% of

P in FA, with a corresponding value of 970 mm $yr^{-1}$. The largest spatial variations between the biomes are for AF, with SD representing 18% of P, while for CT this percentual is of 13%.

As shown in **Figure 3b**, $ET_0$ values follow an inverse tendency for those of P along the year, being the highest mean rates, above 5.0 mm $d^{-1}$, from November (DOY 305) to March (DOY 080) for both biomes, however with higher values for CT. In the middle of the year, the $ET_0$ rates drop to below 3.0 mm $d^{-1}$ in June (DOY 161–176). At the annual scale, the CT biome, with a mean total of 1597 mm $yr^{-1}$ is 3% higher than the corresponding value of 1550 mm $yr^{-1}$ for AF, indicating a general lack of rainfall attending the atmospheric demands. Differences in spatial variations of the atmospheric demands between biomes are small in the middle of the year when occur the lowest SD values of $ET_0$, but outside the rainy season, the highest spatial variations are for AF.

Incident global solar radiation ($R_G$) is the main energy source for water fluxes and for vegetation growth (**Figure 3c**). $R_G$ values also presented an inverse tendency of those for P throughout the year. The highest ones were from November to March (DOY 305 to 064), with 16-day averages above 21.5 MJ $m^{-2}$ $d^{-1}$ for both biomes, which together with the lowest P values, favor water stress conditions. The minimum $R_G$ rates happen during the middle of the year from May to July (DOY 145–192), when the averages stay below 15.5 MJ $m^{-2}$ $d^{-1}$, but under conditions of the highest P. However, low differences arise between biomes, being the average $R_G$ for AF 99% of that for CT. As for $ET_0$, the lowest and the highest $R_G$ spatial differences between biomes are respectively in the middle and at the end of the year, with the largest ones for AF.

Although the tendencies of $T_a$ values follow those for $R_G$ (**Figure 3d**), it is observed a gap regarding their upper and lower limits compared with those for $R_G$, due to the time for the sensible heat flux from the soil to the air. The highest average $T_a$ values, above 26.5 °C are from February (DOY 033) to March (DOY 080), while the lowest ones, below 23.5 °C are between June and August (DOY 177–240). There are no strong thermal differences between biomes, however, as in case of $ET_0$ and $R_G$, the lowest differences on spatial variations occur in the middle of the year and the highest ones during the driest periods, with the largest SD values for AF.

## 3.2. Spatial and temporal conditions of biomass production

**Figure 4** presents the spatial distribution, averages and standard deviations (SD) for BIO, at the annual scale (**Figure 4a**) and for the MODIS 16-day periods (**Figure 4b**), regarding the long-term conditions from 2007 to 2023. Data are classified into AF and CT biomes, within the SEALBA agricultural growing region.

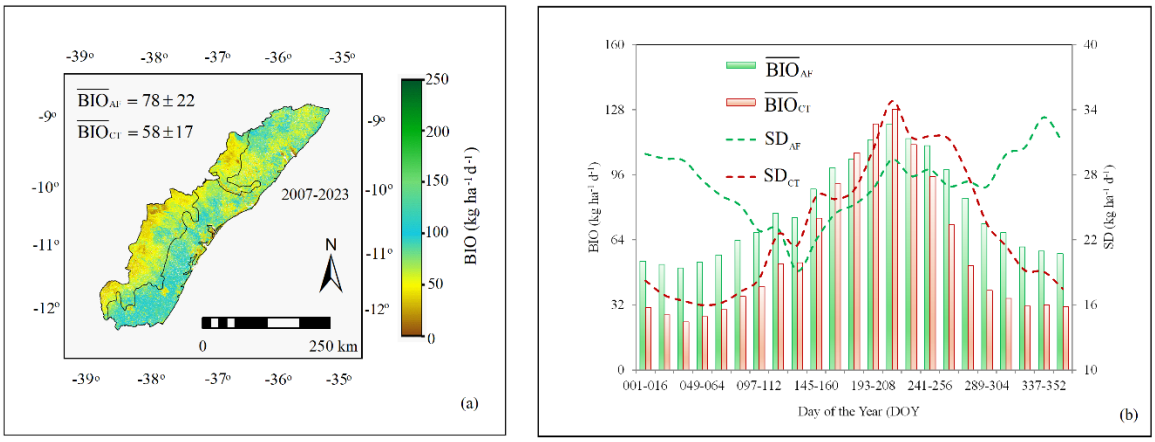


**Figure 4.** Spatial distribution, averages and standard deviations of biomass production (BIO) at the annual scale (**a**) and for the 16-day MODIS images (**b**), considering the long-term conditions for the period from 2007 to 2023, in the biomes Atlantic Forest (AF) and Caatinga (C), within the SEALBA agricultural growing region. Overbars means average pixel values.

According to **Figure 4a,b**, strong spatial and temporal variations on BIO values are observed. From **Figure 4a**, the annual BIO rates in CT are 74% of those for AF, with this last biome presenting lower spatial variation in percentual terms, being SD representing 28% of the mean value, against the corresponding one for CT of 29%.

Considering **Figure 4b**, the highest BIO values happen after the rainy season, from June (DOY 177) to August (DOY 240), with 16-day averages above 100 kg $ha^{-1}$ $d^{-1}$ for both biomes (see also **Figure 3a**). The lowest rates occur at the start of the year, from January to March (DOY 001–064), during the driest period, when the averages are below 50 and 30 kg $ha^{-1}$ $d^{-1}$ in the AF and CT, respectively. At the annual scale, the average BIO in AF of 78 kg $ha^{-1}$ $d^{-1}$ is 34% above of that for CT, with a corresponding mean value of 58 kg $ha^{-1}$ $d^{-1}$.

In the current research, we tested a methodology for detection of anomalies by using the standardized index (STD) for BIO at the annual scale and for the specific 16-day periods of the MOD13Q1 reflectance product, taking the years from 2020 to 2023 as references and considering the long-term periods from 2007–2020, 2007–2021, 2007–2022 and 2007–2023. For these assessments, the average BIO conditions for each of these last years from the data set are first considered at these temporal scales.

**Figure 5** shows the spatial distributions, averages and standard deviations (SD) of the annual average BIO values for the years 2020, 2021, 2022 e 2023, in the AF and CT biomes within the SEALBA agricultural growing region.

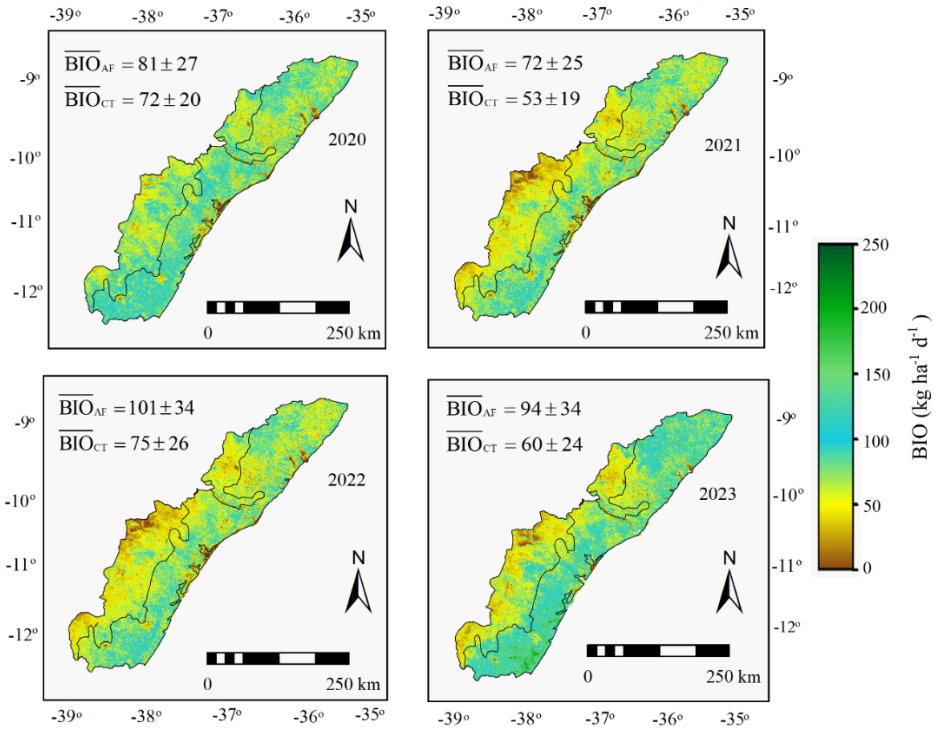


**Figure 5.** Spatial distributions, averages and standard deviations (SD) for the annual values of biomass production (BIO), considering the average conditions for 2020, 2021, 2022 and 2023, in the biomes Atlantic Forest (AF) and Caatinga (CT), within the SEALBA agricultural growing region. Overbars means average pixel values.

According to **Figure 5**, considering all the analyzed years (2020 to 2023), the BIO values for AF were around 13 to 17% of those for CT, with the highest differences between biomes in 2023 while the smallest ones happened in 2020. The lowest BIO rates were in 2021, when the mean pixel value for the region was 63 kg ha$^{-1}$ d$^{-1}$, and the highest ones, averaging 88 kg ha$^{-1}$ d$^{-1}$, happened in 2022, with annual average BIO above 80 kg ha$^{-1}$ d$^{-1}$ in AF and higher than 70 kg ha$^{-1}$ d$^{-1}$ for CT from 2020 to 2022.

Picturing BIO dynamics within each analyzed year, **Figure 6** shows the average pixel values and standard deviations (SD), for the MODIS 16-day periods, from 2020 to 2023, classifying the biomes AF and CT within SEALBA agricultural growing region.

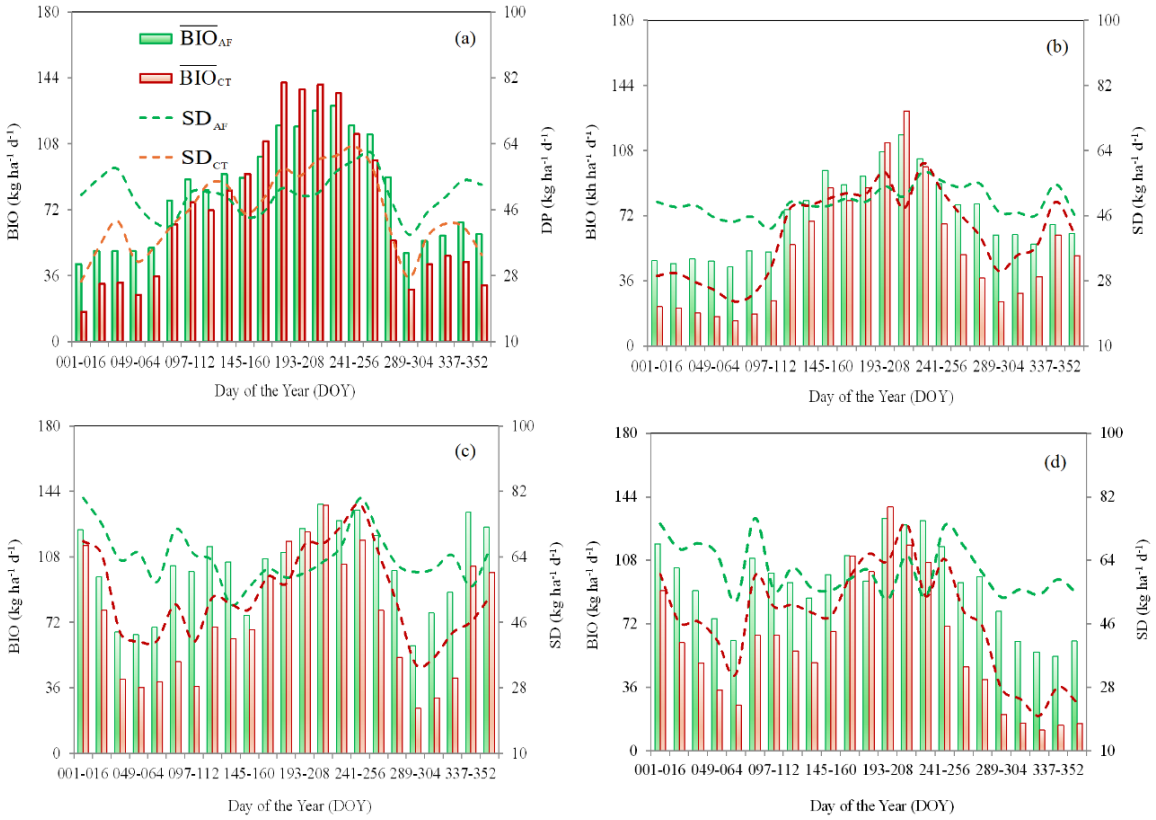


**Figure 6.** Pixel averages and standard deviations (SD) of biomass production (BIO), for the MODIS 16-day periods, during the years 2020 (**a**), 2021 (**b**), 2022 (**c**) and 2023 (**d**), classifying the biomes Atlantic Forest (AF) and Caatinga (CT) within SEALBA, in terms of Day of the Year (DOY). Overbars means average pixel values.

Considering all the analyzed years, from 2020 to 2023 and both biomes, AF and CT, the periods with the highest BIO were from the end of June (DOY 177) to the end of July (DOY 208), when the average rates surpassed 100 kg $ha^{-1}$ $d^{-1}$. The lowest BIO values were concentrated during the driest period (see also **Figure 3a**), with some 16-day average values below 50 kg $ha^{-1}$ $d^{-1}$ for AF and lower than 20 kg $ha^{-1}$ $d^{-1}$ for CT, from 2020 to 2021. Even that in general, BIO values for AF were higher than those for CT, mainly due to better rainfall conditions, there were some short periods with rates for CT similar or higher than those for AF, occurring in situations of no limited root-zone moisture for both biomes.

### 3.3. Standardized index for biomass production

**Figure 7** presents the spatial distributions, averages and standard deviations (SD) of the standardized index (STD) average values for BIO ($BIO_{STD}$) at the annual scale, for the years 2020, 2021, 2022 and 2023, classifying the biomes AF and CT within SEALBA.

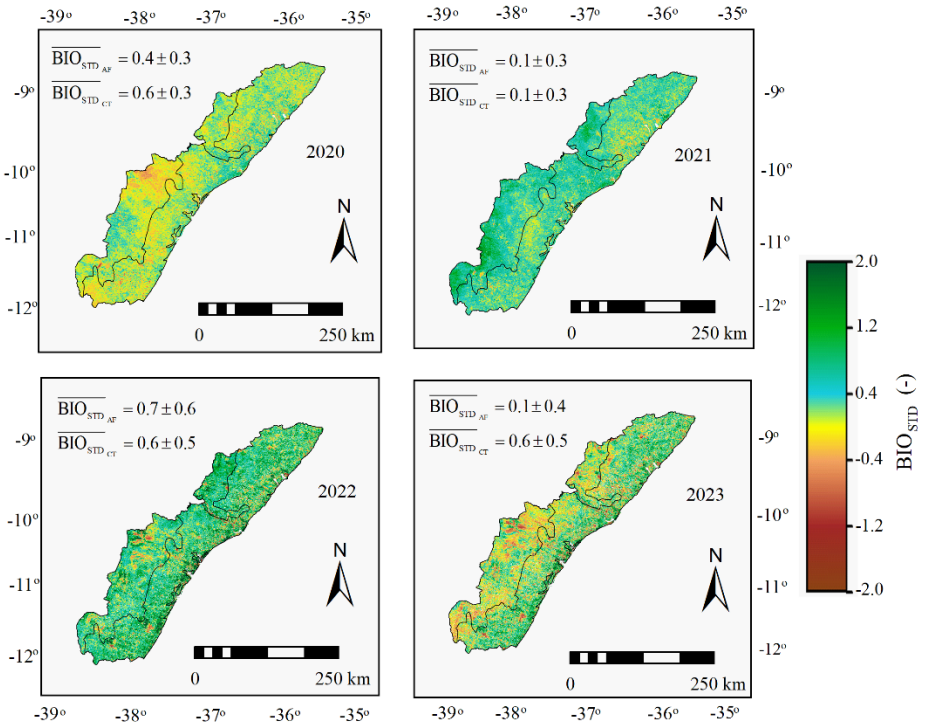


**Figure 7.** Spatial distributions, averages and standard deviations (SD) for the standardized index (STD) for biomass production ($BIO_{STD}$) at the annual scale, for the years 2020, 2021, 2022 and 2023, considering the long-term values from 2007 to each of these years, in the biomes of Atlantic Forest (AF) and Caatinga (CT), within the SEALBA agricultural growing region. Overbars means average pixel values.

The $BIO_{STD}$ values presented in **Figure 7** allow the identification of how much, during the years from 2020 to 2023, at the annual scale, vegetation vigor conditions differ from those of the long-term values (2007–2020, 2007–2021, 2007–2022 and 2007–2023). Higher $BIO_{STD}$ values indicate better vigor conditions, while the lower ones can translate environmental stress [9,21,55] (Leivas et al., 2014; Teixeira et al., 2021; Zhang et al., 2021).

The lowest $BIO_{STD}$ values happened in 2021 for both biomes, AF and CT, with an average of 0.1, indicating vigor of plants like that for the long-term period from 2007 to 2021. In general, the highest values were for AF, with the annual average of 0.7 for this biome in 2022, translating more often conditions of BIO rates above the ones for the long-term period from 2007 to 2022, meaning larger vegetation vigor.

**Figure 8** presents the dynamics of the $BIO_{STD}$ average values, together with the standard deviations (SD), for the MODIS 16-day periods, during the years 2020 to 2023, considering the long-term periods of 2007–2020, 2007–2021, 2007–2022 and 2007–2023, classifying the biomes AF and CT within the SEALBA agricultural growing region.

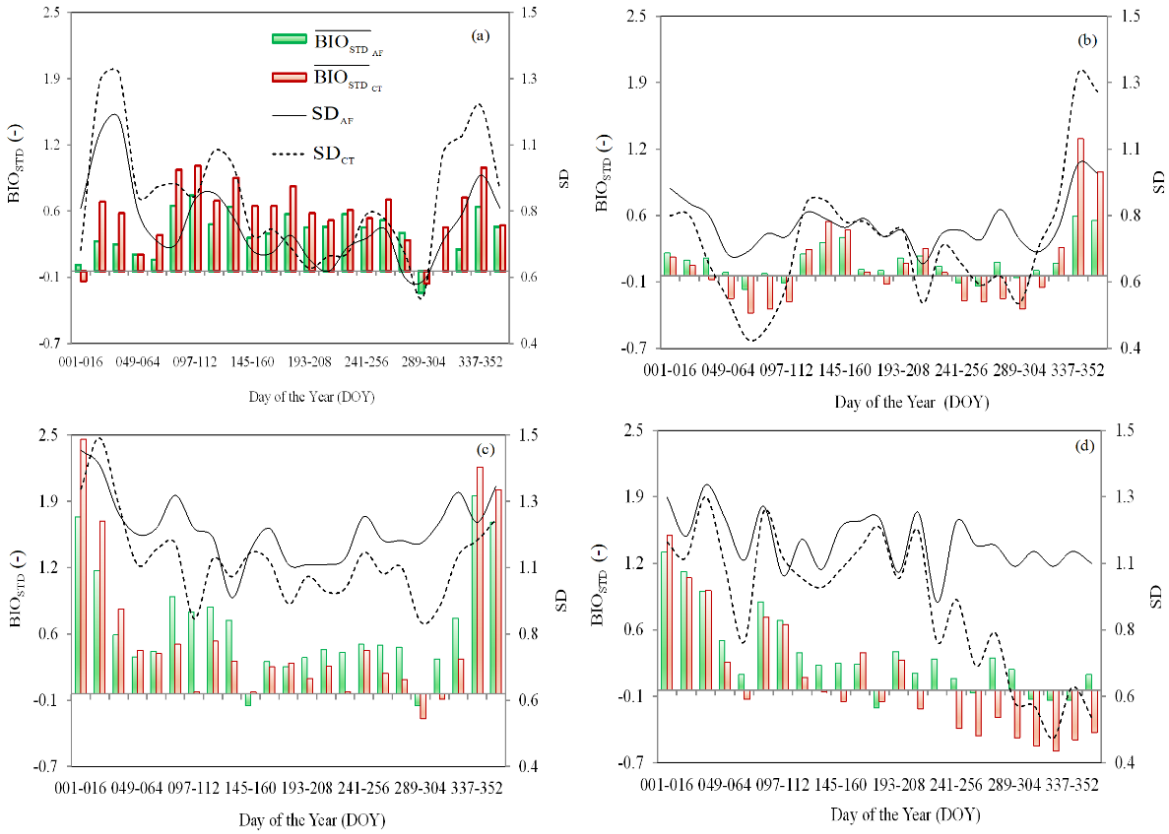


**Figure 8.** Pixel averages of the standardized index (STD) for biomass production ($BIO_{STD}$) and standard deviations (SD), for the MODIS 16-day periods during the years 2020 (**a**), 2021 (**b**), 2022 (**c**) and 2023 (**d**), regarding the long–term conditions of 2007–2020, 2007–2021, 2007–2022 and 2007–2023 in the Atlantic Forest (AF) and Caatinga (CT) biomes within SEALBA, in terms of Day of the Year (DOY). Overbars means average pixel values.

For the year 2020 (**Figure 8a**), the highest positive $BIO_{STD}$ average values were concentrated from March to July (DOY 081–192), in both biomes, AF and CT, meaning higher root-zone moisture and available energy in favor of the vegetative growth for their agroecosystems, regarding the long-term conditions of 2007 to 2020. The negative values happened only at the start of January (DOY 001–016) and in October (DOY 289–304) for both AF and CT, indicating BIO rates below of the long-term ones, meaning poorer vegetation vigor.

Considering the year 2021 and the long-term conditions from 2007 to 2021 (**Figure 8b**), the largest positive average $BIO_{STD}$ values occurred at the end of the year for both biomes, in December (DOY 337–365), reaching to 0.6 in AF and 1.3 in CT, indicating better vegetation vigor conditions, when comparing to the long-term ones. The negative values happened during two periods of the year, from February to April (DOY 033–112) and from June to October (DOY 167–304), for both biomes, evidencing BIO rates below those for the long-term conditions, what could have impacted negatively rainfed agriculture and forestry during these periods.

Analyzing $BIO_{STD}$ for 2022 (**Figure 8c**), one can see few situations of negative 16-day average values for both biomes, AF and CT, occurring only in two periods along the year, reaching to −0.1 and −0.2 in AF and CT, respectively, from May to June (DOY 145–160) and in October (DOY 289–304), meaning the slightly worst vegetation growth conditions, comparing with the those for the long-term periods from

2007 to 2022. However, outside these short periods, high positive $BIO_{STD}$ values occurred, mainly between January and February (DOY 001–048) and in December (DOY 337–365), when the averages were above 1.5, translating better conditions for rainfed agriculture as well as for forest exploration and lower water requirements for irrigated agriculture.

For 2023, regarding the long-term period 2007–2023 (**Figure 8d**), there were several negative $BIO_{STD}$ average values during the second half of the year, most noticed for CT, reaching −0.6, clear evidence of poor vegetative growth. However, several positive ones occurred for AF along the year 2023, mainly during the first half of the year. These results clearly showed the worst conditions for rainfed agriculture and forestry during the second half of the year in CT when compared with the previous analyzed years.

Among the analyzed years, the one with the most negative $BIO_{STD}$ values was 2023, but concentrated in the CT biome, indicating periods with the lowest vegetative growth, when comparing with the long-term conditions from 2007 to 2023. The highest positive $BIO_{STD}$ values were for AF in 2022, picturing high vegetation growth rates, considering the long-term period 2007–2022. The average $BIO_{STD}$ around zero in 2021 indicated that BIO rates during this year were like those for the long-term conditions from 2007 to 2021.

## 4. Discussion

From the processed weather data depicted in **Figure 3**, according to the rainfall dynamics, there are two well-defined seasons, one dry and another rainy, promoting distinct conditions for vegetative growth in both biomes, CT and AF, within the SEALBA agricultural growing region, with the rainiest conditions for AF. On the other hand, the CT biome besides having lower P, presents higher $ET_0$ rates with more aridity conditions in the climatic water balance. $R_G$ and $T_a$ also show an inverse tendency of that for P without significative differences in magnitudes between biomes but with a delay regarding the thermal and solar energy conditions due to the time for the sensible heat flux from the surfaces to the low atmosphere.

Long term BIO values from 2007 to 2023 are higher for AF than for CT, however, even with lower BIO rates in CT, there is a short period, at the end of the rainy season, from June to August (DOY 177–208), when BIO rates for this biome surpass those for AF, showing a larger and quicker response by the CT species to the rainfall water availability in the vegetation root-zones. BIO rates much higher than those for introduced irrigated crops were reported in the semiarid conditions of Northeast Brazil during the climatically driest period of the year [47]. Variations on BIO in AF and CT is most affected by rainfall amounts than by solar radiation levels with a time delay around two months for the maximum BIO values regarding those for P. This delay occurs due to the time for the root-zone to attain good moisture levels for plant growth after rainfalls [9] (Zhang et al. 2021). The general higher BIO for AF along the year is explained by larger rainfall volumes, but under no-limited rainwater conditions, the higher rates in CT during some short periods are due to more available energy [56] (Seneviratne et al. 2010).

BIO assessments from 2020 to 2023, in general, SEALBA represented good conditions for vegetation growth, however with different rates for both biomes along the seasons according to rainfall water availability. Rebello et al. (2020), With MODIS images processing from 2012 to 2015, water stress conditions were detected significantly affecting BIO rates in the AF biome, followed strong recovering of vegetation activities with the start of the rainy season [57]. Applying the SAFER algorithm to MODIS images, [58] found annual average BIO values from 47 to 93 kg $ha^{-1}$ $d^{-1}$ for AF within the São Francisco River basin varying according to moisture conditions, in Northeast Brazil. These previous studies corroborate with our results for the AF biome within SEALBA.

Throughout field measurements from 2014 to 2015 in CT, [34] Silva et al. (2017) reported that the natural species of this biome act as carbon sources to the atmosphere during the driest periods, resulting in lower BIO rates, and as carbon sink during the rainy seasons, promoting higher BIO values. It is also confirmed in [36] that in the CT biome, BIO rates decrease under water stress conditions, resulting in rapid changes on the carbon dynamics, as these situations affect the phenology, seasonality, stomatal conductance and photosynthesis of its natural species. These previous reports show similarity with our results for the CT biome in the SEALBA agricultural growing region.

The highest BIO rates happening during the rainy season for both biomes in the current study, under the best water availability in the vegetation root-zones, agree with other studies under different environmental conditions, in which the association of maximum NDVI values with optimum soil moisture levels were verified [19,22,59] (Vicente-Serrano et al., 2015, 2018; Bento et al., 2018). Positive annual $BIO_{STD}$ average values, for both biomes from 2020 to 2023, indicated that, in general, at this timescale, the root-zone moisture and available energy were in favor of BIO in the SEALBA agricultural growing region. This fact showed general good conditions for rainfed crops as well for forest exploration and less water need for irrigated agriculture, in comparison with those for the long-term periods [9,21] (Teixeira et al. 2021a, Zhang et al. 2021).

From the BIO anomaly assessments, carried out between the years 2020 and 2023, the deviations of vegetation growth from specific periods regarding the long-term conditions could be identified, through the $BIO_{STD}$ values, showing potential support for identification of better planting dates for rainfed agriculture, irrigation water needs for irrigated agriculture and better periods for forestry. The plants vigor can be strongly variable throughout the years, for both, AF and CT biomes within the SEALBA agricultural growing region, without following specific tendencies. Negative $BIO_{STD}$ values can badly impact agriculture while positive ones are favorable for crop growth and forest exploration.

According to [60] Guauque-Melado et al. (2022), distinct biomes respond differently to the water and energy availability for vegetation growth, depending on the weather conditions. In case of the biome CT, its species develop physiological adaptations to overcome environmental stresses [35] (Marques et al., 2020). Detections of anomalies on BIO rates are appropriate for monitoring ecosystems in a sustainable way, as they represent alterations in plant developments, affecting

vegetation productivity [6,8,9,21,61] (Huang et al., 2016; Teixeira et al., 2021; Xu et al., 2013; Yang et al., 2016; Zhang et al., 2019; Zhang et al., 2021).

On the one hand, increasing BIO is important, as its values are related to water consumption, plant growth and crop productivities [9,62] (Seddon et al., 2016; Zhang et al., 2021). On the other hand, a reduction on evapotranspiration rates without compromising BIO but improving the water productivity levels is desirable, because this reduction can contribute for minimizing water conflicts among water users [3] (Teixeira et al., 2023). According to [63] Zhou & Zhou (2009), air humidity and available energy were the most important parameters for the variations on water and vegetation conditions in Northeast China. However, BIO rates in plants under water stress conditions can also be affected by the stomatal regulations [64,65] (Mata-Gonzalez et al., 2005; Mateos et al., 2013), which are strongly noticed in the CT species within the SEALBA agricultural growing region.

## 5. Conclusions

It was confirmed the suitability of using remote sensing and weather data for monitoring the dynamics of biomass production (BIO) and its anomalies on large and different time scales, through standardized indexes (STD) for BIO ($BIO_{STD}$), taking the biomes Atlantic Forest (AF) and Caatinga (CT) within the Brazilian agricultural growing region SEALBA as references, coupling the RUE model and the SAFER algorithm with the MODIS' MOD13Q1 reflectance product and gridded weather data.

From the BIO anomaly assessments for the years 2020, 2021, 2022 and 2023, regarding the long-term periods from 2007 till each of these years, the deviations from the historical conditions could be identified by comparing specific periods with long-term data, showing potential to monitor vegetation growth in mixed agroecosystems. Although significant differences in the energy and thermal conditions did not occur between the analyzed biomes, strong spatial and temporal differences on BIO rates could be detected, caused mainly by distinct rainfall water availability. Rainfall is the main responsible weather parameter driver for the spatial BIO variations, which explains the large differences between CT and AF. It is important to note that varying BIO might also be caused by different areas of soil covered by the vegetation within these biomes, affecting the partitions into transpiration and evaporation. Within SEALBA, higher BIO values are for the AF biome, however CT presents situations with similar or even higher rates just after the rainy seasons, due to the stronger and faster response of its species to variations on the root-zone moisture levels.

Rainfall distribution throughout the year contributed to the magnitude of the evaporative fraction ($ET_f$), representing the root-zone moisture. However, there were gaps between BIO and precipitation, which may be related to the time needed for recovering good conditions of soil moisture after rainfall, but also because some of the rainfall water is lost by runoff and percolation, what also affects BIO. Applications of the standardized index to BIO in this case study showed that this index is useful for monitoring vegetation conditions, having potential to support sustainable environmental management, as it pictures suitable periods and areas for agriculture and forestry, allowing rational vegetation management while minimizing water

competitions by distinct water users, increased by climate and land-use changes, with possibilities for replication of the methods in other environmental conditions.

Although the methods were tested in a specific Brazilian agricultural growing region, the success of the coupled use of MODIS images and gridded weather data showed potential for the implementation of an operational BIO environmental monitoring system by using historical data sets in other environmental conditions, with enough details to differentiate vegetation conditions in distinct biomes. The BIO spatial determinations and their anomalies showed strong potential to support public policies regarding the management and conservation of natural resources, with the possibility for replication of the methods in other countries. Limitations for application of the methods in other environments could be lack of long-term weather data on large scales and the probable need for modelling equation calibrations which will demand simultaneous field and satellite measurements.

**Author contributions:** AA: Running models, water productivity assessments and writing the manuscript, designing figures, result analyses, software resources. AT: Conceptualizations, water productivity assessments and writing the manuscript, result analyses, software resources, and supervision. JL: Downloading and processing satellite images, and formatting weather data, methodology and data curation. CT: Downloading and processing satellite images and weather data, and result analyses. IS: Acted on downloading/processing satellite images and weather data.

**Funding**: This research had no funding received.

**Conflict of interest:** The authors Ana Azevedo, Antônio Teixeira, Inajá Sousa, Janice Leivas, and Celina Takemura declare that they have no known competing financial interests or personal relationships that could have appeared to influence the work reported in this paper.

**Availability of data and materials**: Data and materials will be available on request.

## References

1. Wu C, Munger JW, Niu Z, et al. Comparison of multiple models for estimating gross primary production using MODIS and eddy covariance data in Harvard Forest. Remote Sensing of Environment. 2010; 114(12): 2925–2939. doi: 10.1016/j.rse.2010.07.012
2. Adak T, Kumar G, Chakravarty NVK, et al. Biomass and biomass water use efficiency in oilseed crop (*Brassica juncea* L.) under semi-arid microenvironments. Biomass and Bioenergy. 2013; 51: 154–162. doi: 10.1016/j.biombioe.2013.01.021
3. Teixeira A, Leivas J, Takemura C, et al. Remote sensing environmental indicators for monitoring spatial and temporal dynamics of water and vegetation conditions: applications to the Brazilian biomes. Environmental Monitoring and Assessment. 2023; 195: 944. doi: 10.21203/rs.3.rs-2573923/v1
4. Yan H, Fu Y, Xiao X, et al. Modeling gross primary productivity for winter wheat–maize double cropping system using MODIS time series and $CO_2$ eddy flux tower data. Agriculture, Ecosystems & Environment. 2009; 129(4): 391–400. doi: 10.1016/j.agee.2008.10.017
5. Bayma G, Nogueira SF, Adami M, et al. Estimating forage mass in Brazilian pasture-based livestock production systems through satellite and climate data integration. Computers and Electronics in Agriculture. 2025; 237: 110496. doi: 10.1016/j.compag.2025.110496
6. Yang Y, Guan H, Batelaan O, et al. Contrasting responses of water use efficiency to drought across global terrestrial ecosystems. Scientific Reports. 2016; 6(1). doi: 10.1038/srep23284

7. Zhang X, Zhang B. The responses of natural vegetation dynamics to drought during the growing season across China. Journal of Hydrology. 2019; 574: 706–714. doi: 10.1016/j.jhydrol.2019.04.084
8. Zhang L, Qiao N, Huang C, et al. Monitoring Drought Effects on Vegetation Productivity Using Satellite Solar-Induced Chlorophyll Fluorescence. Remote Sensing. 2019; 11(4): 378. doi: 10.3390/rs11040378
9. Zhang G, Su X, Singh VP, et al. Appraising standardized moisture anomaly index (SZI) in drought projection across China under CMIP6 forcing scenarios. Journal of Hydrology: Regional Studies. 2021; 37: 100898. doi: 10.1016/j.ejrh.2021.100898
10. Almeida SLH de, Souza JBC, Nogueira SF, et al. Forage Mass Estimation in Silvopastoral and Full Sun Systems: Evaluation through Proximal Remote Sensing Applied to the SAFER Model. Remote Sensing. 2023; 15(3): 815. doi: 10.3390/rs15030815
11. Santos JEO, Cunha FF da, Filgueiras R, et al. Performance of SAFER evapotranspiration using missing meteorological data. Agricultural Water Management. 2020; 233: 106076. doi: 10.1016/j.agwat.2020.106076
12. Zhang B, Wu Y, Zhao B, et al. Progress and Challenges in Intelligent Remote Sensing Satellite Systems. IEEE Journal of Selected Topics in Applied Earth Observations and Remote Sensing. 2022; 15: 1814–1822. doi: 10.1109/jstars.2022.3148139
13. Shi X, Elmore A, Li X, et al. Using spatial information technologies to select sites for biomass power plants: A case study in Guangdong, China. Biomass Bioenergy. 2008; 32: 35–43. doi: 10.1016/j.biombioe.2007.06.008
14. Molden D, Bin D, Loeve R, et al. Agricultural water productivity and savings: policy lessons from two diverse sites in China. Water Policy. 2007; 9(S1): 29–44. doi: 10.2166/wp.2007.043
15. Clementini C, Pomente A, Latini D, et al. Long-Term Grass Biomass Estimation of Pastures from Satellite Data. Remote Sensing. 2020; 12(13): 2160. doi: 10.3390/rs12132160
16. Chen Y, Guerschman J, Shendryk Y, et al. Estimating Pasture Biomass Using Sentinel-2 Imagery and Machine Learning. Remote Sensing. 2021; 13(4): 603. doi: 10.3390/rs13040603
17. Rampazo NAM, Picoli MCA, De Castro Teixeira AH, et al. Water Consumption Modeling by Coupling MODIS Images and Agrometeorological Data for Sugarcane Crops. Sugar Tech. 2020; 23(3): 524–535. doi: 10.1007/s12355-020-00919-7
18. Beguería S, Vicente-Serrano SM, Reig F, et al. Standardized precipitation evapotranspiration index (SPEI) revisited: parameter fitting, evapotranspiration models, tools, datasets and drought monitoring. International Journal of Climatology. 2014; 34: 3001–3023. doi: 10.1002/joc.3887
19. Bento VA, Gouveia CM, DaCamara CC, et al. A climatological assessment of drought impact on vegetation health index. Agricultural and Forest Meteorology. 2018; 259: 286–295. doi: 10.1016/j.agrformet.2018.05.014
20. Gouveia CM, Trigo RM, Beguería S, et al. Drought impacts on vegetation activity in the Mediterranean region: An assessment using remote sensing data and multi-scale drought indicators. Global and Planetary Change. 2017; 151: 15–27. doi: 10.1016/j.gloplacha.2016.06.011
21. Teixeira AH de C, Leivas JF, Pacheco EP, et al. Biophysical Characterization and Monitoring Large-Scale Water and Vegetation Anomalies by Remote Sensing in the Agricultural Growing Areas of the Brazilian Semi-Arid Region. Advances in Remote Sensing for Natural Resource Monitoring. Wiley Online Library; 2021. pp. 94–109. doi: 10.1002/9781119616016.ch7
22. Vicente-Serrano SM, Miralles DG, Domínguez-Castro F, et al. Global Assessment of the Standardized Evapotranspiration Deficit Index (SEDI) for Drought Analysis and Monitoring. Journal of Climate. 2018; 31(14): 5371–5393. doi: 10.1175/jcli-d-17-0775.1
23. Kim D, Rhee J. A drought index based on actual evapotranspiration from the Bouchet hypothesis. Geophysical Research Letters. 2016; 43(19). doi: 10.1002/2016gl070302
24. Brouwers NC, van Dongen R, Matusick G, et al. Inferring drought and heat sensitivity across a Mediterranean forest region in southwest Western Australia: a comparison of approaches. Forestry. 2015; 88(4): 454–464. doi: 10.1093/forestry/cpv014
25. Peters AJ, Walter-Shea EA, Ji L, et al. Drought monitoring with NDVI-based standardized vegetation index. Photogrammetric Engineering & Remote Sensing. 2002; 68(1): 71–75.
26. Hao Z, AghaKouchak A. Multivariate Standardized Drought Index: A parametric multi-index model. Advances in Water Resources. 2013; 57: 12–18. doi: 10.1016/j.advwatres.2013.03.009
27. Zhang Y, Xiao X, Zhou S, et al. Canopy and physiological controls of GPP during drought and heat wave. Geophysical Research Letters. 2016; 43(7): 3325–3333. doi: 10.1002/2016gl068501
28. Ceschia E, Béziat P, Dejoux JF, et al. Management effects on net ecosystem carbon and GHG budgets at European crop sites. Agriculture, Ecosystems & Environment. 2010; 139(3): 363–383. doi: 10.1016/j.agee.2010.09.020

29. Zhao M, Running SW. Drought-Induced Reduction in Global Terrestrial Net Primary Production from 2000 Through 2009. Science. 2010; 329(5994): 940–943. doi: 10.1126/science.1192666
30. Lewinsohn TM, Prado PI. How Many Species Are There in Brazil? Conservation Biology. 2005; 19(3): 619–624. doi: 10.1111/j.1523-1739.2005.00680.x
31. Mariano DA, Santos CAC dos, Wardlow BD, et al. Use of remote sensing indicators to assess effects of drought and human-induced land degradation on ecosystem health in Northeastern Brazil. Remote Sensing of Environment. 2018; 213: 129–143. doi: 10.1016/j.rse.2018.04.048
32. Ribeiro MC, Metzger JP, Martensen AC, et al. The Brazilian Atlantic Forest: How much is left, and how is the remaining forest distributed? Implications for conservation. Biological Conservation. 2009; 142(6): 1141–1153. doi: 10.1016/j.biocon.2009.02.021
33. Santos MG, Oliveira MT, Figueiredo KV, et al. Caatinga, the Brazilian dry tropical forest: can it tolerate climate changes? Theoretical and Experimental Plant Physiology. 2014; 26(1): 83–99. doi: 10.1007/s40626-014-0008-0
34. Silva PF da, Lima JR de S, Antonino ACD, et al. Seasonal patterns of carbon dioxide, water and energy fluxes over the Caatinga and grassland in the semi-arid region of Brazil. Journal of Arid Environments. 2017; 147: 71–82. doi: 10.1016/j.jaridenv.2017.09.003
35. Marques TV, Mendes K, Mutti P, et al. Environmental and biophysical controls of evapotranspiration from Seasonally Dry Tropical Forests (Caatinga) in the Brazilian Semiarid. Agricultural and Forest Meteorology. 2020; 287: 107957. doi: 10.1016/j.agrformet.2020.107957
36. Pereira D dos R, Mello CR de, Silva AM da, et al. Evapotranspiration and estimation of aerodynamic and stomatal conductance in a fragment of Atlantic Forest in mantiqueira range region, MG. CERNE. 2010; 16(1): 32–40. doi: 10.1590/s0104-77602010000100004
37. Teixeira AH de C, Bastiaanssen WGM, Ahmad MD, et al. Analysis of energy fluxes and vegetation-atmosphere parameters in irrigated and natural ecosystems of semi-arid Brazil. Journal of Hydrology. 2008; 362(1–2): 110–127. doi: 10.1016/j.jhydrol.2008.08.011
38. Reinermann S, Asam S, Kuenzer C. Remote sensing of grassland production and management A review. Remote Sensing. 2020; 12: 1949. doi: 10.3390/rs12121949.
39. Claverie M, Demarez V, Duchemin B, et al. Maize and sunflower biomass estimation in southwest France using high spatial and temporal resolution remote sensing data. Remote Sensing of Environment. 2012; 124: 844–857. doi: 10.1016/j.rse.2012.04.005
40. Tesfaye K, Walker S, Tsubo M. Radiation interception and radiation use efficiency of three grain legumes under water deficit conditions in a semi-arid environment. European Journal of Agronomy. 2006; 25(1): 60–70. doi: 10.1016/j.eja.2006.04.014
41. Monteith JL. Climate and the efficiency of crop production in Britain. Philosophical Transactions of the Royal Society of London B, Biological Sciences. 1977; 281(980): 277–294. doi: 10.1098/rstb.1977.0140
42. Zhao M, Heinsch FA, Nemani RR, et al. Improvements of the MODIS terrestrial gross and net primary production global data set. Remote Sensing of Environment. 2005; 95(2): 164–176. doi: 10.1016/j.rse.2004.12.011
43. Bastiaanssen WGM, Ali S. A new crop yield forecasting model based on satellite measurements applied across the Indus Basin, Pakistan. Agriculture, Ecosystems & Environment. 2003; 94: 321–340. doi: 10.1016/S0167-8809(02)00034-8
44. Nyolei D, Nsaali M, Minaya V, et al. High resolution mapping of agricultural water productivity using SEBAL in a cultivated African catchment, Tanzania. Physics and Chemistry of the Earth, Parts A/B/C. 2019; 112: 36–49. doi: 10.1016/j.pce.2019.03.009
45. Zwart SJ, Bastiaanssen WGM, de Fraiture C, et al. WATPRO: A remote sensing based model for mapping water productivity of wheat. Agricultural Water Management. 2010; 97(10): 1628–1636. doi: 10.1016/j.agwat.2010.05.017
46. Teixeira AH de C. Determining Regional Actual Evapotranspiration of Irrigated Crops and Natural Vegetation in the São Francisco River Basin (Brazil) Using Remote Sensing and Penman-Monteith Equation. Remote Sensing. 2010; 2(5): 1287–1319. doi: 10.3390/rs0251287
47. Teixeira AH de C, Scherer-Warren M, Hernandez F, Andrade R, Leivas J. Large-Scale Water Productivity Assessments with MODIS Images in a Changing Semi-Arid Environment: A Brazilian Case Study. Remote Sensing. 2013; 5(11): 5783–5804. doi: 10.3390/rs5115783
48. Consoli S, Vanella D. Comparisons of satellite-based models for estimating evapotranspiration fluxes. Journal of Hydrology. 2014; 513: 475–489. doi: 10.1016/j.jhydrol.2014.03.071

49. Procopio SDO, Cruz MAS, de Almeida MRM, et al. SEALBA: Região de Alto Potencial Agrícola no Nordeste Brasileiro. Embrapa Tabuleiros Costeiros; 2019. p. 62.
50. Francisquini MI, Lorente FL, Ruiz Pessenda LC, et al. Cold and humid Atlantic Rainforest during the last glacial maximum, northern Espírito Santo state, southeastern Brazil. Quaternary Science Reviews. 2020; 244: 106489. doi: 10.1016/j.quascirev.2020.106489
51. Almagro A, Oliveira PTS, Nearing MA, et al. Projected climate change impacts in rainfall erosivity over Brazil. Scientific Reports. 2017; 7(1). doi: 10.1038/s41598-017-08298-y
52. Allen RG, Pereira LS, Raes D, et al. Crop Evapotranspiration, Guidelines for Computing Crop Water Requirements. FAO irrigation and drainage paper 56. FAO; 1998.
53. de Bruin HAR. From Penman to Makkink. In: Hooghart JC (editors). Proceedings and Information: TNO Committee on Hydrological Sciences. Gravenhage; 1987. Volume 39. pp. 5–31.
54. Venancio LP, Mantovani EC, Amaral CH do, et al. Evapotranspiration mapping of commercial corn fields in Brazil using SAFER algorithm. Scientia Agricola. 2021; 78(4). doi: 10.1590/1678-992x-2019-0261
55. Leivas JF, Andrade RG, Victoria DDC, et al. Monitoramento da seca 2011/2012 no nordeste brasileiro a partir do satélite spot-vegetation e TRMM. Agricultural Engineering. 2014; 22(3): 211–221. doi:10.13083/1414-3984.v22n03a03.
56. Seneviratne SI, Corti T, Davin EL, et al. Investigating soil moisture–climate interactions in a changing climate: A review. Earth-Science Reviews. 2010; 99(3–4): 125–161. doi: 10.1016/j.earscirev.2010.02.004
57. Rebello VPA, Getirana A, Rotunno Filho OC, et al. Spatiotemporal vegetation response to extreme droughts in eastern Brazil. Remote Sensing Applications: Society and Environment. 2020; 18: 100294. doi: 10.1016/j.rsase.2020.100294
58. Teixeira AH de C, Takemura CM, Leivas JF, et al. Water productivity monitoring by using geotechnological tools in contrasting social and environmental conditions: Applications in the São Francisco River basin, Brazil. Remote Sensing Applications: Society and Environment. 2020; 18: 100296. doi: 10.1016/j.rsase.2020.100296
59. Vicente-Serrano S, Cabello D, Tomás-Burguera M, et al. Drought Variability and Land Degradation in Semiarid Regions: Assessment Using Remote Sensing Data and Drought Indices (1982–2011). Remote Sensing. 2015; 7(4): 4391–4423. doi: 10.3390/rs70404391
60. Guauque-Mellado D, Rodrigues A, Terra M, et al. Evapotranspiration under Drought Conditions: The Case Study of a Seasonally Dry Atlantic Forest. Atmosphere. 2022; 13(6): 871. doi: 10.3390/atmos13060871
61. Huang J, Yu H, Guan X, et al. Accelerated dryland expansion under climate change. Nature Climate Change. 2015; 6(2): 166–171. doi: 10.1038/nclimate2837
62. Seddon AW, Macias-Fauria M, Long PR, et al. Sensitivity of global terrestrial ecosystems to climate variability. Nature. 2016; 531: 229–232. doi: 10.1038/nature16986
63. Zhou L, Zhou G. Measurement and modelling of evapotranspiration over a reed (Phragmites australis) marsh in Northeast China. Journal of Hydrology. 2009; 372(1–4): 41–47. doi: 10.1016/j.jhydrol.2009.03.033
64. Mata-González R, McLendon T, Martin DW. The Inappropriate Use of Crop Transpiration Coefficients (Kc) to Estimate Evapotranspiration in Arid Ecosystems: A Review. Arid Land Research and Management. 2005; 19(3): 285–295. doi: 10.1080/15324980590951469
65. Mateos L, González-Dugo MP, Testi L, et al. Monitoring evapotranspiration of irrigated crops using crop coefficients derived from time series of satellite images. I. Method validation. Agricultural Water Management. 2013; 125: 81–91. doi: 10.1016/j.agwat.2012.11.005